Stability of the Tree of Shapes to Additive Noise

Nicolas Boutry & Guillaume Tochon

EPITA Research and Development Lab. (LRDE), Le Kremlin-Bicêtre, France
`surname.name@lrde.epita.fr`

Abstract. The tree of shapes (ToS) is a famous self-dual hierarchical structure in mathematical morphology, which represents the inclusion relationship of the shapes (*i.e.* the interior of the level lines with holes filled) in a grayscale image. The ToS has already found numerous applications in image processing tasks, such as grain filtering, contour extraction, image simplification, and so on. Its structure consistency is bound to the cleanliness of the level lines, which are themselves deeply affected by the presence of noise within the image. However, according to our knowledge, no one has measured before how resistant to (additive) noise this hierarchical structure is. In this paper, we propose and compare several measures to evaluate the stability of the ToS structure to noise.

Keywords: Tree of shapes, additive noise, stability, tree distance

1 Introduction

The tree of shapes (ToS) is a morphological hierarchical representation which encodes the inclusion relationship between the shapes (*i.e.*, the interior of the level lines with holes filled) in a given image. Initially proposed by [20], it has then been extensively studied, both for its theoretical [1,10,13] and computational [8,14] properties, as well as its wide range of applications in image processing (such as image segmentation [7] and simplification [26], object detection and extraction [19], morphological filtering [24], shape-space representations [25,18]), morphological attribute profiles computation [16], feature extraction for image retrieval [4], and curve matching [22]).

It is usually considered as the fusion between the max-tree [23] and its dual, the min-tree. Being a morphological representation, the ToS structure relies on the existence of a total ordering between the pixel values (to order by inclusion the level lines of the image), hence its existence for grayscale images (although it has been successfully adapted to multichannel images [9]). Therefore, the potential presence of noise within the image appears as a critical question regarding the cleanliness of the level lines, and thus the stability and the significance of the ToS representation with respect to the image it is built upon. More specifically, the fact that level lines would tend to degrade as the signal-to-noise ratio in the image decreases comes with the intuition that the resulting ToS also loses relevance (at least for most of the shapes it contains). Measuring 1) how far from the "clean" ToS lies the "noisy" ToS (*i.e.*, the ToS built on the image corrupted

by noise) and 2) how much the shapes of the "noisy" ToS have been degraded by the presence of noise could give some useful insights on the image content as well as the credibility that should be given to further processing applied on the ToS (such as image segmentation or object recognition resulting from it).

Unfortunately, the ToS stability has not been really explored yet in the mathematical morphology community. A study of the robustness of common hierarchical structures in terms of pixel classification performances of some morphological attribute profiles has been carried out in [16], leading to the conclusion that the ToS, the min/max trees and the ω-tree show superior performance compared to the α-tree depending of the choice of some threshold. In [4], it is shown that the MSER feature extractor can be significantly improved using the tree of shapes for some image retrieval tasks, due to an addition estimated to between 20% and 40% of features. This tree-based measure is robust to noise since it is derived from the MSER methodology, but no ToS robustness measure is given. In [22], an approach based on curve matching is proposed which is rotation-invariant and seems to be robust to noise (although this property is not emphasized in the cited work). Clearly, these three papers are not motivated by the idea of giving a complementary toolbox of robustness/stability measures as deeply as we do in the present paper.

When it comes to measuring distances between tree graphs, possible solutions encompasses tree-edit distances [3], graph distances [6], treelets based on graph kernels [12], Reeb graphs distances [2], or interleaving distances between merge trees [21]. However, the ToS structure is richer than a simple graph since all nodes also bear an image-related meaning that should also be taken into account to evaluate the similarity between such structures (for instance, two ToS might contain very different shapes even though their graph structure is the same). In this paper, the aim is to proceed to a very exploratory research, which concerns the definition of mathematical tools able to measure *how much a ToS is perturbed* when we add noise in the image it comes from (see Figure 1). The plan is the following: Section 2 recalls the mathematical background necessary to understand the paper, Sections 3, 4, 5 and 6 present spectral, topological, and geometrical measures of the stability of a ToS to added noise, and Section 7 concludes the paper with a summary of the different measures presented in the paper and their properties (variance, type of convergence, monotonicity, slope around 0, and so on). In the appendix (Section A), we add material about preliminary results on natural images, we show elementary measures computed on synthetic/natural images, and we show the evolution of a tree of shape on natural/synthetic images when noise amplitude increases.

2   Mathematical background about the tree of shapes

We begin by briefly recalling the way the ToS is computed (see Figure 2). Starting from a given image $I : \Omega \to \mathbb{R}$, we can compute for each possible level $\ell \in \mathbb{R}$ the upper threshold sets: $[I \geq \ell] = \{x \in \Omega \; ; \; I(x) \geq \ell\}$, and the lower threshold sets: $[I < \ell] = \{x \in \Omega \; ; \; I(x) < \ell\}$. Using these sets, we compute their connected
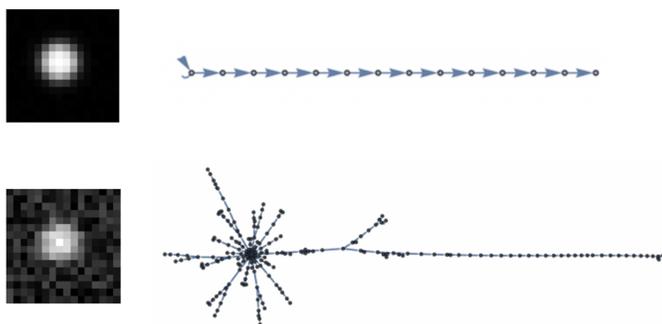
Fig. 1. In the raster scan order, a synthetic image without noise, its tree of shapes, the noisy version of this image, and its tree of shapes (we used an additive noise). The aim of this paper is to provide measures of these perturbations at the hierarchical level, taking account (or not) of the shapes of the respective trees.
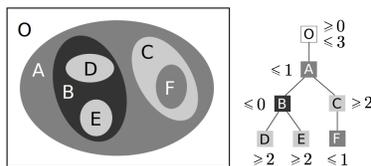

Fig. 2. An example of tree of shapes computation from [14]

components in Ω and we saturate them (using the cavity fill-in operator), to obtain the upper shapes: $\mathcal{S}_\geq = \{Sat(\Gamma) \; ; \; \Gamma \in \mathcal{CC}([I \geq \ell])\}$, and the lower shapes: $\mathcal{S}_< = \{Sat(\Gamma) \; ; \; \Gamma \in \mathcal{CC}([I < \ell])\}$. By merging the sets $\mathcal{S}_\geq$ and $\mathcal{S}_<$, and assuming that the image is well-composed [5], we obtain the so-called *tree of shapes* $\mathcal{T}$ of I. It is known to be self-dual and contrast-invariant, and this way it represents the inclusion relationship between the shapes in the image.

3 Proposed spectral measures

After a brief recall in matter of Hausdorff and spectral distances, we propose four candidate spectral distances to measure stability of the ToS to additive noise.

3.1 Mathematical preliminaries

The Hausdorff distance Let N be some positive integer. Let h be a mapping from $\mathbb{R} \times \mathbb{R}^N$ to $\mathbb{R}$ such as for any $v \in \mathbb{R}$ and $E \in \mathbb{R}^N$: $h(v, E) = \min_{e \in E} |v - e|$. We can define the Hausdorff distance [15] on two sets E_1, E_2 of N scalars by:

$$\mathcal{HA}(E_1, E_2) = \max \left(\max_{e_1 \in E_1} h(e_1, E_2), \max_{e_2 \in E_2} h(e_2, E_1) \right).$$

Fig. 3. The original image (maximum pixel intensity = 100) and noisy versions ($\zeta = 20$, $\zeta = 50$ and $\zeta = 100$).
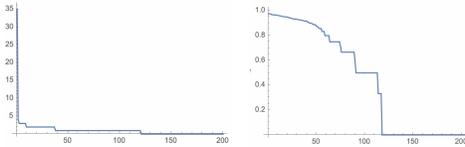

Fig. 4. Spectra of a ToS when the adjacency is weighted by zeros/ones (left) and by the IoU (right). We can see that the spectrum on the right side has more relief thanks to the IoU.

The co-spectral distance Given two trees $\mathcal{T}$ and $\mathcal{T}'$, let us assume that we want to measure their difference based on their spectrum, more exactly on the spectrum of the Laplacian [11] of the adjacency matrix of these trees considered as graphs. Starting from a tree $\mathcal{T}$, we can compute its adjacency matrix $\mathcal{A}$, which is defined as $\mathcal{A}_{i,j} = \mathcal{A}_{j,i} = 1$ if the node j is connected with the node i in $\mathcal{T}$, otherwise $\mathcal{A}_{i,j} = \mathcal{A}_{j,i} = 0$. Using this adjacency matrix, we can compute the Laplacian of $\mathcal{A}$, denoted $\mathcal{L}$, which is defined by the formula: $\mathcal{L} = \mathcal{D} - \mathcal{A}$, where $\mathcal{D}$ is the degree matrix [11] of $\mathcal{A}$. Based on these definitions[1], the co-spectral distance between two trees $\mathcal{T}$ and $\mathcal{T}'$ with the same number of nodes N is defined as $\sum_{i \in [1,N]} (\lambda_i - \lambda_i')^2$, where $\Lambda = \{\lambda_i\}_{i \in [1,N]}$ (resp. $\Lambda' = \{\lambda_i'\}_{i \in [1,N]}$) is the spectrum of the Laplacian matrix $\mathcal{L}$ (resp. $\mathcal{L}'$) of $\mathcal{T}$ (resp. $\mathcal{T}'$).

3.2   Proposed spectral-based distances

We start from the ToS $\mathcal{T}$ corresponding to a given image $I : \Omega \rightarrow \mathbb{N}$ (see Figure 3). Given some $\zeta \in \mathbb{N}$, we add an independent noise n which follows a uniform discrete law on $[\![0, \zeta]\!]$ so that $I' = n + I$, and we compute its ToS $\mathcal{T}'$. ζ is said to be the noise amplitude.

In this section, we use the following methodology:

$$I \rightarrow \mathcal{T} \rightarrow \mathcal{A} \rightarrow \mathcal{L} \rightarrow \Lambda .$$

First approach Let $\mathcal{T}$ and $\mathcal{T}'$ be two ToS computed on images I and I', respectively. We consider the adjacency matrices deduced from these ToS by

---

[1] We recall that the spectrum of the Laplacian of a graph does not depend on the enumeration of its nodes, which explains why we can establish measures on the spectra of two graphs to compute a "distance" between them.
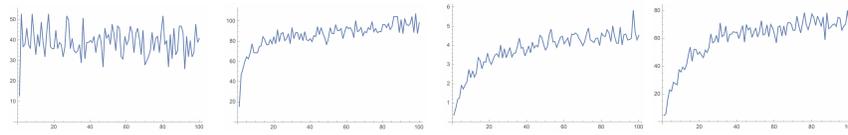
Fig. 5. From left to right, computation of μ_1, μ_2, μ_3 and μ_4 as a function of the noise amplitude ranging from 0 to 100 (the amplitude of the initial image).

setting $\mathcal{A}_{i,j}$ to 1 when $\mathcal{S}_j$ is parent of $\mathcal{S}_i$ (otherwise we write 0), and we compute the spectra of their respective Laplacians Λ and Λ' (see Figure 4 (left)). Then, we compute the Hausdorff distance applied to Λ and Λ' to define our first measure:

$$\mu_1(\Lambda, \Lambda') = \mathcal{H}\mathcal{A}(\Lambda, \Lambda').$$

Observation: We can observe in Figure 5 (left) that this distance does not increase with the amplitude of the additive noise, leading to the conclusion that this measure does not seem well-suited for stability estimation. Indeed, we expect the function to be increasing with the noise amplitude to represent that the higher the noise, the more perturbed (thus the farther away) the "noisy" ToS.

Second approach Due to the failure of μ_1, we reconsider the Hausdorff formula for stability estimation and investigate the following measure:

$$\mu_2(\Lambda, \Lambda') = \mathcal{H}\mathcal{A}_{mod}(\Lambda, \Lambda') = \max\left(\sum_{\lambda \in \Lambda} h(\lambda, \Lambda'), \sum_{\lambda' \in \Lambda'} h(\lambda', \Lambda)\right).$$

The aim of μ_2 is to consider all the eigenvalues that have been inserted in the new spectrum: the more they differ from the initial ones (or the more numerous they are), the higher their impact. At the same time, we want to ensure that if no new eigenvalue is introduced, then the stability measure is zero.

Observation: The first thing we can remark (see Figure 5 left middle) is that it is monotonic (in mean). A second remark is that the slope of μ_2 seems to be high for low noise amplitudes. This is normal since the structure of the ToS is modified (many new branches are inserted and initial branches are elongated) even for very small values of ζ, in particular for synthetic images like the one under study.

Third approach We did not consider in the previous approaches the shapes of the two trees $\mathcal{T}$ and $\mathcal{T}'$. We propose then to add this information in the adjacency matrix by setting $\mathcal{A}_{i,j}$ as the intersection over union (IoU) value of $\mathcal{S}_i$ and $\mathcal{S}_j$ when $\mathcal{S}_j$ is parent of $\mathcal{S}_i$, otherwise we set it to zero. We then obtain the spectra depicted in Figure 4 (right). Following, we compute between the two new spectra Λ_{IoU} and Λ'_{IoU} the formula:

$$\mu_3(\mathcal{T}, \mathcal{T}') = \mathcal{H}\mathcal{A}_{mod}(\Lambda_{IoU}, \Lambda'_{IoU}).$$
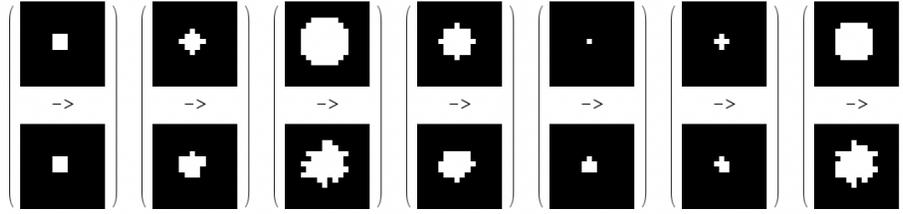
Fig. 6. Example of matching obtained using the HMA: the (initial) shapes extracted from $\mathcal{T}$ depicted in the first row are associated by the HMA to the (noisy) shapes extracted from $\mathcal{T}'$ depicted in the second row.

Observation: We observe in Figure 5 (right) that μ_3 increases slower than μ_2 and then is less sensible to the high perturbation that the ToS undergoes. Furthermore, the monotonic behavior of μ_2 is preserved.

Fourth Approach Being in the case where we can have spectra of different sizes, we propose now to extend the usual definition of co-spectral distance in the following manner. We start from the discrete spectra Λ_{IoU} and Λ'_{IoU} and then interpolate them in a linear way. We obtain $\mathscr{I}_{IoU}$ and $\mathscr{I}'_{IoU}$, respectively. Since they are continuous, we can easily resize them to obtain two signals with a same support $[1, \max(N, N')]$ where N is the size of Λ and N' is the size of Λ'. This leads to our new measure:

$$\mu_4(\mathcal{T}, \mathcal{T}') = \int_1^{\max(N,N')} \left(\mathscr{I}_{IoU}(t) - \mathscr{I}'_{IoU}(t) \right)^2 dt.$$

Observation: The results of this measure can be observed in the rightmost panel of Figure 5, which shows a much satisfying measure in the sense that it keeps increasing as long as $\mathcal{T}$ is perturbed.

Conclusion about the spectral approaches: Taking into account the IoU in the coefficients of the adjacency matrix allows us to obtain a more stable Laplacian spectrum but needs more computations. We recommend then μ_2 for fast computations, and μ_3 or μ_4 for more stable stability evaluation.

4   Proposed elongation measure

Let us assume that we have as usual our two trees $\mathcal{T}$ and $\mathcal{T}'$ computed from two images $I : \Omega \to \mathbb{R}$ and $I' : \Omega \to \mathbb{R}$, respectively. We now apply the Hungarian Matching Algorithm [17] (HMA) on these two tree of shapes based on the IoU measure computed on their shapes (we do not consider the structure of the trees but only their shapes since the tree structure can be induced by the set of shapes

of each image). In this way, the pairing cost between two shapes $\mathcal{S} \in \mathcal{T}$ and $\mathcal{S}' \in \mathcal{T}'$ is IoU$(\mathcal{S}, \mathcal{S}')$, and the final optimal matching $\mathcal{H}$ is defined as the injective function f from $\mathcal{T}$ to $\mathcal{T}'$ which maximizes the total cost:

$$\mathcal{H} = \arg\min{}_{f \text{ injective}} \sum_{\mathcal{S} \in \mathcal{T}} (1 - \text{IoU}(\mathcal{S}, f(\mathcal{S}))).$$

Note that usually, we use the HMA on sets of same cardinality, or on squared matrices. In our case, we use a bipartite graph $\mathcal{A}$ with the rows corresponding to the initial tree $\mathcal{T}$, the columns corresponding to the final (noisy) tree $\mathcal{T}'$, and each $\mathcal{A}_{i,j}$ represents the (position-sensitive) pairing cost between the ith shape of $\mathcal{T}$ and the jth shape of $\mathcal{T}'$ (see Figure 6). Now that we have our matching between the shapes of $\mathcal{T}$ and a subset $\mathcal{H}(\mathcal{T})$ of $\mathcal{T}'$, we can compute the elongation measure ℓ of $\mathcal{T}'$ relatively to $\mathcal{T}$ for any shape in $\mathcal{T}'$ in the following manner. When $\mathcal{S}'$ equals Ω, we define $\ell(\mathcal{S}') = 0$ (since this shape never moves in the ToS). Then, for any shape $\mathcal{S}' \in \mathcal{H}(\mathcal{T}) \backslash \{\Omega\}$, we compute its inverse image $\mathcal{H}^{-1}(\mathcal{S}')$ by the HMA. Now, we compute its parent $\text{Par}_{\mathcal{T}}(\mathcal{H}^{-1}(\mathcal{S}'))$. We are ensured that this parent exists since in the tree of shapes, any shape has a parent (Ω is its own parent). Then, we compute its image $\mathfrak{P}(\mathcal{S}') := \mathcal{H}(\text{Par}_{\mathcal{T}}(\mathcal{H}^{-1}(\mathcal{S}')))$ in $\mathcal{T}'$. After having defined:

$$\ell_0(\mathcal{S}') = \text{depth}_{\mathcal{T}'}(\mathcal{S}') - \text{depth}_{\mathcal{T}'}(\mathfrak{P}(\mathcal{S}')) - 1,$$

the value:

$$\ell(\mathcal{S}') = \max(0, \ell_0(\mathcal{S}'))$$

is then a measure of how much the tree has been elongated from a local point of view for a given shape of $\mathcal{H}(\mathcal{T})$.

Let us remark that it can happen that $\ell_0(\mathcal{S}')$ is negative. Indeed, the HMA ensures optimality in matters of costs, but does not guarantee that $\mathfrak{P}(\mathcal{S}')$ is a parent of $\mathcal{S}'$ by following the procedure described above (even if we observed experimentally in simple cases that it is almost always the case). Let us recall however that, even if the HMA is optimal, the given pairing solution is not always unique, so this measure depends on the matching result. In the case where we want to obtain a scalar measure of the elongation, we proceed the following way. First we estimate the number of shapes of $\mathcal{H}(\mathcal{T})$ whose elongation is positive: $N' = \text{Card}(\{\mathcal{S}' \in \mathcal{H}(\mathcal{T}) \; ; \; \ell_0(\mathcal{S}') \geq 0\})$. Then, if N' is equal to zero, we consider that the total elongation is zero. Otherwise, it is equal to:

$$\ell_{tot}(\mathcal{T}, \mathcal{T}') = \frac{1}{N'} \sum_{\mathcal{S}' \in \mathcal{H}(\mathcal{T}) \text{ s.t. } \ell_0(\mathcal{S}') \geq 0} \ell_0(\mathcal{S}').$$

Observation: Despite its high variance as soon as we reach values next to $\zeta = 30$ (see Figure 7), and then its non effectiveness as measure of the stability of the tree of shapes for high noise amplitudes, this measure remains the only proposed topological measure and is thus worthy of existence.
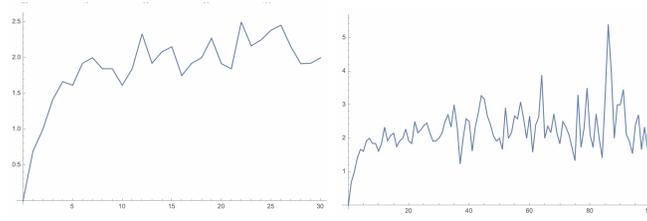
Fig. 7. Total elongation ℓ_{tot} as a function of the noise amplitude. On the left side, we show the elongation for noises whose amplitude goes from 0 to 30, and on the right side, from 0 to 100. We can remark that when the noise amplitude reaches about 30% of the signal amplitude, the measure converges in mean but its variance increases dramatically.

5   Proposed deformation measure $\mathcal{M}$

Let us assume that we have the same hypotheses as usual on the trees $\mathcal{T}$ and $\mathcal{T}'$ and that we apply the HMA on their sets of shapes. We have a matching between $\mathcal{T}$ and $\mathcal{H}(\mathcal{T})$ from which we can compute the first part of our measure:

$$\mathcal{M}_1(\mathcal{T}, \mathcal{T}') := \sum_{\mathcal{S} \in \mathcal{T}} d_{\mathrm{IoU}}(\mathcal{S}, \mathcal{H}(\mathcal{S})),$$

with $d_{\mathrm{IoU}}(\mathcal{S}, \mathcal{S}') = 1 - \mathrm{IoU}(\mathcal{S}, \mathcal{S}')$ their Jaccard index. The term $\mathcal{M}_1(\mathcal{T}, \mathcal{T}')$ measures how much the shapes of $\mathcal{T}$ have been deformed due to the added noise. Now, we have also to consider the intermediary shapes which have been added in-between the initial shapes. For this aim, we define for $A, B \in \mathcal{T}'$ with $A \supset B$:

$$\mathrm{Interm}_{\mathcal{T}'}(A, B) = \{\mathcal{S} \in \mathcal{T}' \; ; \; A \supset \mathcal{S} \supset B\}$$

Using this last notation, we can define the set of intermediary shapes in $\mathcal{T}'$:

$$\mathcal{I} = \{\mathcal{S}' \in \mathcal{T}' \; ; \; \exists A', B' \in \mathcal{H}(\mathcal{T}), A' \supset \mathcal{S}' \supset B'\} = \bigcup_{A, B \in \mathcal{H}(\mathcal{T})} \mathrm{Interm}_{\mathcal{T}'}(A, B).$$

Since the common domain Ω to I and I' (parent of every shape $\mathcal{S}$ in $\mathcal{T}$ and every shape $\mathcal{S}'$ in $\mathcal{T}'$) always belong to $\mathcal{H}(\mathcal{T})$, we can simplify $\mathcal{I}$:

$$\mathcal{I} = \bigcup_{\mathcal{S}' \in \mathcal{H}(\mathcal{T})} \mathrm{Parents}_{\mathcal{T}'}(\mathcal{S}') \setminus \mathcal{H}(\mathcal{T}),$$

where $\mathrm{Parents}_{\mathcal{T}'}(\mathcal{S}')$ is the set of strict parents of $\mathcal{S}'$ in $\mathcal{T}'$.
Once we have processed the matching shapes in $\mathcal{T}'$, some shapes remain (the ones which do not match at all with the initial tree). For them, we consider the measure:

$$\mathcal{M}_2(\mathcal{T}, \mathcal{T}') = \sum_{\mathcal{S}' \in \mathcal{T}' \setminus \mathcal{H}(\mathcal{T}) \setminus \mathcal{I}} \min_{\mathcal{S} \in \mathcal{T}} d_{\mathrm{IoU}}(\mathcal{S}', \mathcal{S}).$$
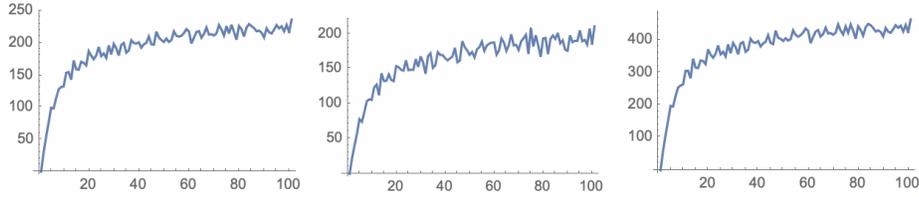
Fig. 8. From left to right, $\mathcal{M}_1$, $\mathcal{M}_2$, and $\mathcal{M}_{\text{tot}}$ with α_1 and α_2 are arbitrarily chosen equal to one.

This measure shows how much the little shapes perturb the global structure of the tree. We finally conclude with the total measure of the deformation between $\mathcal{T}$ and $\mathcal{T}'$:

$$\mathcal{M}_{\text{tot}}(\mathcal{T}, \mathcal{T}') := \alpha_1 \mathcal{M}_1(\mathcal{T}, \mathcal{T}') + \alpha_2 \mathcal{M}_2(\mathcal{T}, \mathcal{T}'),$$

with $\{\alpha_i\}_{i \in [1,2]}$ a set of non-zero positive parameters. We can remark that when $\mathcal{T} = \mathcal{T}'$, we obtain $\mathcal{M}_{\text{tot}}(\mathcal{T}, \mathcal{T}') = 0$.

Observation: In Figure 8, we can remark that $\mathcal{M}_1$ and $\mathcal{M}_2$ seem to have the same behavior when ζ increases. The main remark on the total measure is that it does not suffer from the limitation of the elongation measure presented in the previous section, and then seems to us to be a good candidate to quantify noise in a hierarchical structure like the ToS.

6   Proposed measure β based on d_{IoU}-matching

Assuming we have the same notations as usual, we propose now to compute measures based on d_{IoU} (and not anymore using the HMA). In other words, we do what we call d_{IoU}-*matching*. Let us first define the following function $\xi : \mathcal{T} \to \mathcal{T}'$ as:

$$\xi(\mathcal{S}) := \arg \min_{\mathcal{S}' \in \mathcal{T}'} d_{\text{IoU}}(\mathcal{S}, \mathcal{S}')$$

This mapping represents the closest shape (in the d_{IoU} sense) of $\mathcal{S}$ in $\mathcal{T}'$. For the sake of simplicity, let us define for any tree $\mathcal{T}_0$:

$$\mathcal{P}_{\mathcal{T}_0}(k) := \big\{ \mathcal{S} \in \mathcal{T}_0 \text{ s.t. depth}_{\mathcal{T}_0}(\mathcal{S}) = k \big\}$$

Once we have this mapping and this notation, we can define a measure based on the intersection over union using the same mapping ξ:

$$\beta(k) := \frac{1}{\text{Card}\left(\mathcal{P}_{\mathcal{T}}(k)\right)} \sum_{\mathcal{S} \in \mathcal{P}_{\mathcal{T}}(k)} d_{\text{IoU}}(\mathcal{S}, \xi(\mathcal{S})).$$

Note that we tested also its dual version by switching $\mathcal{T}$ and $\mathcal{T}'$ in this formula but the results were not relevant as a stability estimator.
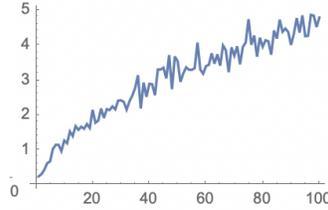
Fig. 9. The measure $\beta^\forall$ as a function of the noise amplitude ζ for $\zeta \in [1, 100]$.

Fig. 10. Summary of the different properties of each approach on the toy-image. Note that the representative slowness $\mathfrak{s}$ in the interval of low noise amplitudes is measured by the value of ζ at which the curve reaches the 50% of its maximum on the interval $[1, 100]$ for the first time.

	Type	Asymp. conv.	Monotonic	$\mathfrak{s}$	HMA-based	d_{IoU}-based	Variance
μ_1	Spectral	Yes	No	1	No	No	High
μ_2	Spectral	Yes	Yes	3	No	No	Small
μ_3	Spectral	Yes	Yes	13	No	No	Small
μ_4	Spectral	Yes	Yes	20	No	No	Small
ℓ_{tot}	Topological	No	No	46	Yes	No	High
$\mathcal{M}_1$	Geometrical	Yes	Yes	10	Yes	No	Small
$\mathcal{M}_2$	Geometrical	Yes	Yes	10	Yes	No	Small
$\beta^\forall$	Geometrical	No	Yes	26	No	Yes	Small

β represents how much the shapes at depth k in $\mathcal{T}$ are perturbed, and we effectively observed that the higher the noise amplitude, the more d_{IoU} tends to one, since the IoU surely tends to zero.

In order to obtain (like in the previous sections) a quantification of the perturbation of the tree of shapes relatively to the noise amplitude, we propose then to compute the sum of the terms β over the possible depths of the components. We obtain then:

$$\beta^\forall = \sum_{k \in [0, \mathrm{depth}(\mathcal{T})]} \beta(k)$$

which is depicted in Figure 9.

Observation: In fact, this is the first measure we found among all our experiments which increases very slowly at the beginning, and furthermore which increases as long as ζ does so. Nevertheless, at excessively high noise amplitudes ($\zeta \geq 180$), the variance of β becomes too high and is not representative anymore.

7   Conclusion

Thanks to our exploratory research, we have been able to propose many measures of how much a tree of shapes is robust to noise. These measures can be geometrical

(based on the shapes and the deformation of their contours), topological (based on the depth of the tree of shapes of an image), or spectral (based on the eigenvalues of the Laplacian of the tree of shapes). Furthermore, theses experiments are symptomatic of the difficulty to efficiently measure a phenomenon which can seem intuitively simple. Indeed, considering the behavior on the interval $[1, 100]$ where 100 is the amplitude of the signal, the only measure which has a low variance, is monotonic, and which does not converges asymptotically (three quality criteria according to us), is the last proposed measure β, that we estimate being the default measure any user should choose in a general context. Table 10 summarizes the main properties of each of our formulas. As future work, we will investigate our measures on different types of hierarchical representations and noise models, on a larger benchmark of natural images to strengthen the provability of our observations.

References

1. Ballester, C., Caselles, V., Monasse, P.: The tree of shapes of an image. ESAIM: Control, Optimisation and Calculus of Variations **9**, 1–18 (2003)
2. Bauer, U., Ge, X., Wang, Y.: Measuring distance between Reeb graphs. In: Proceedings of the thirtieth annual symposium on Computational geometry. pp. 464–473 (2014)
3. Bille, P.: A survey on tree edit distance and related problems. Theoretical computer science **337**(1-3), 217–239 (2005)
4. Bosilj, P., Kijak, E., Lefèvre, S.: Beyond MSER: Maximally Stable Regions using tree of shapes. In: British Machine Vision Conference (2015)
5. Boutry, N., Géraud, T., Najman, L.: A tutorial on well-composedness. Journal of Mathematical Imaging and Vision **60**(3), 443–478 (2018)
6. Bunke, H., Shearer, K.: A graph distance metric based on the maximal common subgraph. Pattern Recognition Letters **19**(3-4), 255–259 (1998)
7. Cardelino, J., Randall, G., Bertalmio, M., Caselles, V.: Region based segmentation using the tree of shapes. In: 2006 International Conference on Image Processing. pp. 2421–2424. IEEE (2006)
8. Carlinet, E., Crozet, S., Géraud, T.: The tree of shapes turned into a max-tree: a simple and efficient linear algorithm. In: 2018 25th IEEE International Conference on Image Processing (ICIP). pp. 1488–1492. IEEE (2018)
9. Carlinet, E., Géraud, T.: MToS: A tree of shapes for multivariate images. IEEE Transactions on Image Processing **24**(12), 5330–5342 (2015)
10. Caselles, V., Monasse, P.: Geometric description of images as topographic maps. Springer (2009)
11. Chung, F.R., Graham, F.C.: Spectral graph theory. No. 92, American Mathematical Soc. (1997)
12. Gaüzere, B., Brun, L., Villemin, D.: Two new graphs kernels in chemoinformatics. Pattern Recognition Letters **33**(15), 2038–2047 (2012)
13. Géraud, T., Carlinet, E., Crozet, S.: Self-duality and digital topology: links between the morphological tree of shapes and well-composed gray-level images. In: Proceedings of the International Symposium on Mathematical Morphology. pp. 573–584. Springer (2015)

14. Géraud, T., Carlinet, E., Crozet, S., Najman, L.: A quasi-linear algorithm to compute the tree of shapes of n-D images. In: Proceedings of the International Symposium on Mathematical Morphology. pp. 98–110. Springer Berlin Heidelberg (2013)
15. Huttenlocher, D.P., Klanderman, G.A., Rucklidge, W.J.: Comparing images using the Hausdorff distance. IEEE Transactions on pattern analysis and machine intelligence **15**(9), 850–863 (1993)
16. Koç, S.G., Aptoula, E., Bosilj, P., Damodaran, B.B., Dalla Mura, M., Lefevre, S.: A comparative noise robustness study of tree representations for attribute profile construction. In: 2017 25th Signal Processing and Communications Applications Conference (SIU). pp. 1–4. IEEE (2017)
17. Kuhn, H.W.: The hungarian method for the assignment problem. Naval research logistics quarterly **2**(1-2), 83–97 (1955)
18. Le Duy Huynh, N.B., Géraud, T.: Connected filters on generalized shape-spaces. Pattern Recognition Letters **128**, 348–354 (2019)
19. Lê Duy Huynh, Y.X., Géraud, T.: Morphology-based hierarchical representation with application to text segmentation in natural images. In: Proceedings of the International Conference on Pattern Recognition. pp. 4029–4034
20. Monasse, P., Guichard, F.: Fast computation of a contrast-invariant image representation. IEEE Transactions on Image Processing **9**(5), 860–872 (2000)
21. Morozov, D., Beketayev, K., Weber, G.: Interleaving distance between merge trees. Discrete and Computational Geometry **49**(22-45), 52 (2013)
22. Pan, Y., Birdwell, J.D., Djouadi, S.M.: Preferential image segmentation using trees of shapes. IEEE Transactions on Image Processing **18**(4), 854–866 (2009)
23. Salembier, P., Oliveras, A., Garrido, L.: Antiextensive connected operators for image and sequence processing. IEEE Transactions on Image Processing **7**(4), 555–570 (1998)
24. Xu, Y., Géraud, T., Najman, L.: Morphological filtering in shape spaces: Applications using tree-based image representations. In: Proceedings of the International Conference on Pattern Recognition. pp. 485–488. IEEE (2012)
25. Xu, Y., Géraud, T., Najman, L.: Connected filtering on tree-based shape-spaces. IEEE transactions on pattern analysis and machine intelligence **38**(6), 1126–1140 (2015)
26. Xu, Y., Géraud, T., Najman, L.: Hierarchical image simplification and segmentation based on Mumford-Shah-salient level line selection. Pattern Recognition Letters **83**, 278–286 (2016)

A   Appendix

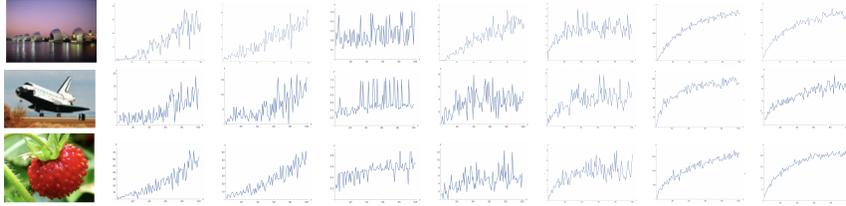## A.1   Preservation of the behavior of our measures on natural images

Fig. 11. From left to right, the studied image and the computations of μ_1, μ_2 , μ_3, μ_4, ℓ, $\mathcal{M}$ and β on three natural images.

The main difference with synthetic images is that natural images show a stronger variance (see Figure 11). Conversely, the behavior of our measures are preserved except for μ_1 which becomes relevant on natural images.

A.2   Preservation of the behavior of our measures on natural images

Fig. 12. Images and their depth, number of nodes, and maximal degrees as a function of the noise amplitude.
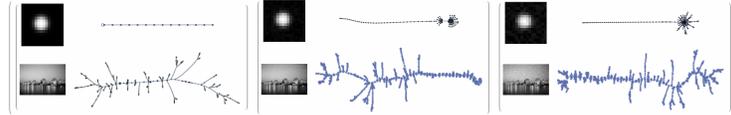

Fig. 13. Ramifications appear in the tree of shapes as long as we add noise to the represented image.

As we can observe in Figures 12 and 13, elementary measures such as depth, numbers of nodes, and maximal degrees are not sufficient to measure the robustness of the ToS structure to noise.